Available online at www.sciencedirect.com
SCIENCE DIRECT®
Carbohydrate Research 340 (2005) 827–833
Carbohydrate RESEARCH

Determining the crystal structure of cellulose III_I by modeling

Zakhia M. Ford,[a,b] Edwin D. Stevens,[a] Glenn P. Johnson[b] and Alfred D. French[b,*]

[a]*Department of Chemistry, University of New Orleans, New Orleans, LA 70124, USA*
[b]*Southern Regional Research Center, US Department of Agriculture, PO Box 19687, New Orleans, LA 70179-0687, USA*

Received 15 October 2004; accepted 21 January 2005

Dedicated to Professor David A. Brant

Abstract—Recently, a one-chain monoclinic unit cell for cellulose III_I having $P2_1$ symmetry and a single glucose in the asymmetric unit was proposed, based on high-resolution diffraction patterns. The new work challenged a two-chain structure that was published 25 years earlier, although it did not provide new three-dimensional coordinates. Our goals were to solve the structure by modeling, find whether modeling would reject the previously determined two-chain unit cell, and compare the model with the anticipated experimental structure. Combinations of three rotamers of the O-2, O-3, and O-6 hydroxyl groups produced 27 'up' and 27 'down' starting structures. Clusters ('minicrystals') of 13 cellotetraose chains terminated by methyl groups for each of the 54 starting structures were optimized with MM3(96). Hydroxyl groups on 16 of these 54 structures reoriented to give very similar hydrogen-bonding schemes in the interiors, along with the lowest energies. Hydrogen bonds included the usual intramolecular O-3H···O-5′ linkage, with O-6′ also accepting from O-3H. Interchain hydrogen bonds form an infinite, cooperative O-6H···O-2H···O-6 network. Direct comparison of total minicrystal energies for the one- and two-chain unit cell was inappropriate because the two-chain cell's alternate chains are shifted 0.9 Å along the *z*-axis. To get comparable energy values, models were built with both cellotetraose and cellohexaose chains. The differences in their energies represent the energies for the central layers of cellobiose units. The one-chain cell models had much lower energy. The eight best 'up' one-chain models agree reasonably well with the structure newly determined by experiment.

Keywords: Carbohydrate; Packing; Polysaccharide; Fiber; Molecular mechanics

1. Introduction

Cellulose was the first carbohydrate to be studied by computer modeling. In 1960, Jones[1] used standard bond lengths, angles, and interatomic distances to construct models that were used as part of a mostly unsuccessful attempt to solve the crystal structure of ramie cellulose I from fiber-diffraction data. The advantages of the method were clear, however, and since then, computer models have been an integral part of most fiber-diffraction studies that seek to determine the atomic positions.[2] Augmentation of crystal structure determinations by modeling is often necessary because the small number of diffraction intensities from most fibers is inadequate to determine the *x*, *y*, and *z*-coordinates of all unique atoms in the structure. With a combined approach, diffraction data can provide some guidance and the modeling energy calculations supply the rest of the information. This approach has been taken to the logical extreme of attempting to solve structures of small organic molecules by modeling with no specific experimental data whatsoever.[3] Those efforts are as yet not sufficiently reliable for general use, but are at the forefront of modeling development.

As modeling has become more sophisticated, methods for experimental study of crystalline fibers have also improved. New sources of highly-crystalline cellulose have been identified, and the preparation of films of oriented

* Corresponding author. Address: 1100 Robert E. Lee Boulevard, New Orleans, LA 70124, USA. Tel.: +1 504 286 4410; fax: +1 504 286 4217; e-mail: afrench@srrc.ars.usda.gov

0008-6215/$ - see front matter © 2005 Elsevier Ltd. All rights reserved.
doi:10.1016/j.carres.2005.01.028

crystallites allows the use of these crystallites, regardless of their initial lack of orientation.[4] Neutron-diffraction work has yielded the details of the hydrogen-bond networks and very powerful synchrotron X-ray beams provide more diffraction data than laboratory generators. Together, the new techniques have resulted in sufficient data that high-resolution, model-free structure determinations of cellulose structures could, in principle, be carried out.

High-resolution structures are now available for cellulose Iα[5] and Iβ,[6] as well as cellulose II.[7] Most native cellulose is a mixture of the Iα and Iβ structures, with the Iα form being prevalent in cellulose that is produced by algae and bacteria, whereas Iβ is dominant in higher plants. The sample for the high-resolution study of cellulose II was produced by treating native cellulose I from flax with 23% NaOH, followed by rinsing and drying. Cellulose II can also be prepared by precipitation from solution, as in the manufacture of rayon, and by bacteria that are either mutants or at low temperature. A third major form, cellulose III, results from treatment with amines that are subsequently evaporated or rinsed off. Although their diffraction patterns are similar, subtle differences distinguish cellulose III that is made starting with cellulose I (III_I) from that starting with cellulose II (III_{II}). Finally, cellulose IV can be prepared by heating the other forms in glycerol at 260 °C. Recently, Wada et al. proposed that IV_I is actually Iβ with lateral disorder.[8]

In 2001, Wada et al. proposed that cellulose III_I has a single-chain monoclinic unit cell with $P2_1$ symmetry and that the O-6 atoms were in the *gt* orientation.[9] Those results contradict a 1976 determination by Sarko et al., who had done a complete analysis based on limited X-ray diffraction data.[10] Their work was based on a two-chain unit cell and determined the O-6 groups to be in *tg* orientations. Although the pattern of Wada et al. has more than 100 intensities, they did not, in that work, attempt to solve the structure. Instead, the O-6 position was determined by accompanying NMR studies. Their results presented a unique opportunity. A modeling study could be independently carried out with an unknown cellulose fiber that would inevitably be determined at high resolution. If successful, it was hoped that our project would encourage the incorporation of higher-quality modeling methods in fiber-diffraction studies. These combined methods would continue to be of use on less-crystalline samples. Of course, a successful prediction would lend credibility to modeling studies on other materials such as amorphous cellulose, for which experimental data are limited and more difficult to interpret.

The high-resolution experimental study of cellulose III has now been published,[11] and we can also compare those results with ours, which were presented at two meetings.[12]

2. Methods

Given the results from Wada et al. regarding the O-6 position and unit-cell dimensions and symmetry,[9] only the hydroxyl group orientations remain as explicit variables. Chem-X was used to construct cellotetraose molecules having twofold screw-axis symmetry and capped with methyl groups at the reducing and non-reducing ends to prevent the formation of unrealistic hydrogen bonds. The O-2, O-3, and O-6 hydroxyl groups on the tetraose models were placed in each of the three staggered orientations (Fig. 1), so that they made torsion angles of −60°, 60°, and 180° with the H-2, H-3, and C-5 atoms. Thus, there were 27 combinations of hydroxyl orientations. These models were placed visually in the unit cell according to Figure 5 in Wada et al.,[9] in both the 'up' and 'down' orientations,[13,14] for a total of 54 starting models. There was substantial confidence in the orientation presented by Wada since it was based on the report by Sarko et al.[10] That orientation would depend on the very strong *hk*0 reflections and is likely to be unaffected by other errors in the determination. Symmetry operators within Chem-X were used to generate clusters (minicrystals) with 13 chains, similar to previous designs,[15] as shown in Figure 2. These 54 minicrystals were then each energy minimized with MM3(96), using a dielectric constant of 3.5 and the hydrogen-bonding potential from MM3(92). We have found that those modifications result in better model crystal structures. No constraints, symmetry operators, or periodic boundaries were placed on the structure during minimization. The plan was to observe the resulting energies and hydrogen-bonding schemes and to select one or more likely structures for comparison with the two-chain structure from Sarko et al.

The minicrystal method is subject to uncontrolled edge effects[16] regarding the positions of the external atoms. However, it has the advantage that it can readily provide energies that are based on a variety of different

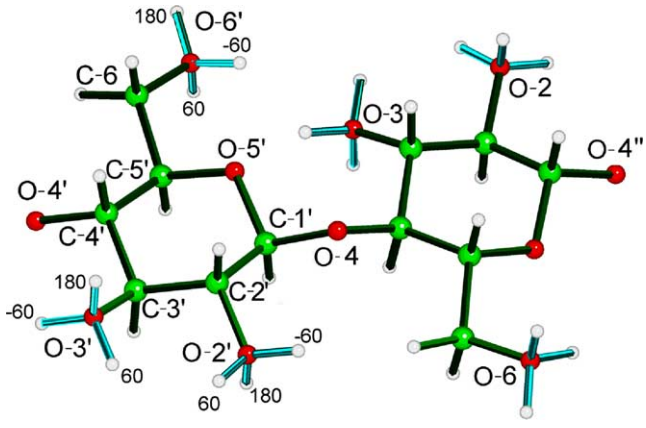

Figure 1. Cellobiose unit with the hydroxyl groups oriented in the 180°, −60°, and +60° orientations.

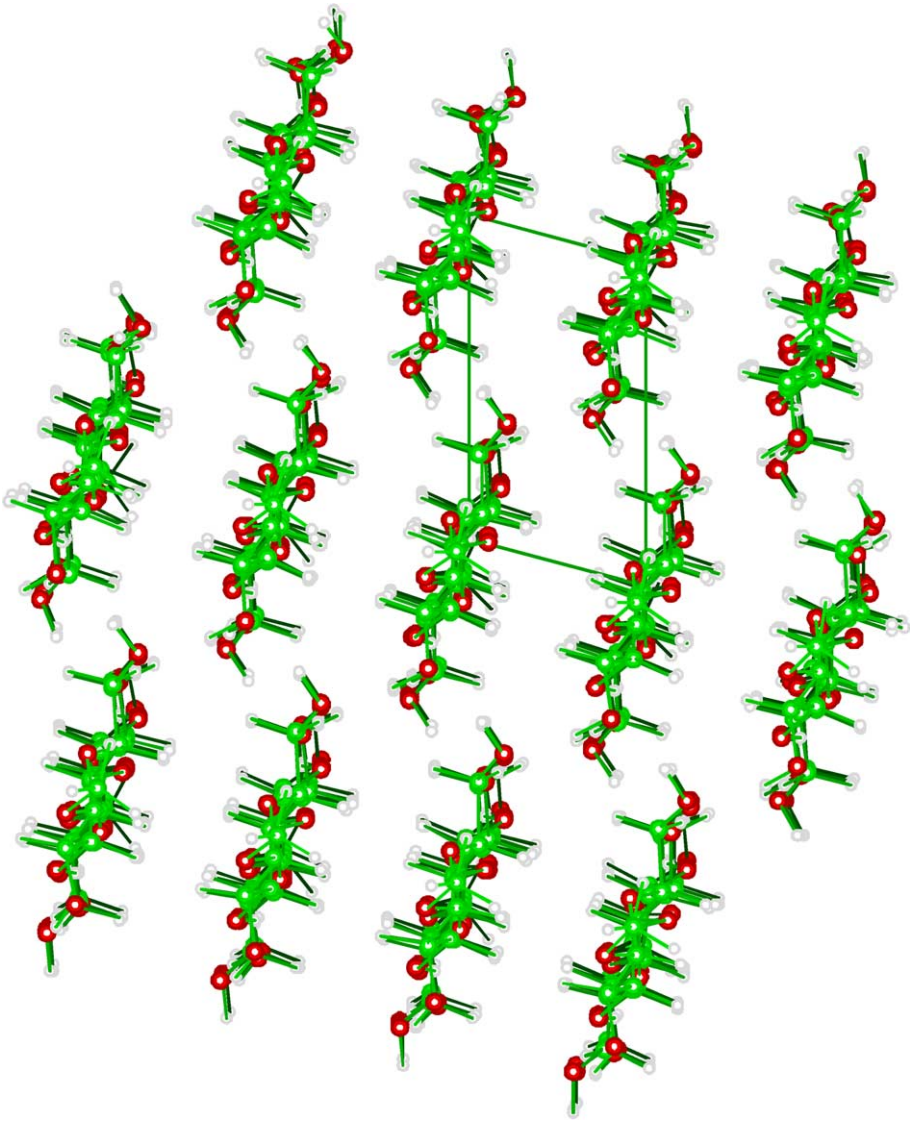

Figure 2. Minicrystal of cellulose III after energy minimization with MM3(96), viewed from above down the long molecular axes, which are parallel to the crystallographic *c*-axis. At the edges of the minicrystal, there is some visible variation in hydrogen position that resulted from different amounts of atom movement during minimization because the atoms have different environments than those in the interior of the minicrystal.

potential-energy functions, including MM3, which is known to reproduce a number of phenomena related to carbohydrates. All energies are reported as kcal/mol of the structures in question. Thus, the energies reported for the tetraose-based minicrystals would be kilocalories for a mole of minicrystals. Other energies reported include kcal/mol of hexaose-based minicrystals and kcal/mol of a layer of cellobiose residues inside the hexaose-based minicrystal. These energies are reported below simply as kcal.

3. Results and discussion

Of the 54 models based on single-chain unit cells, 16 gave total minimized steric energies that were between 237 and 246 kcal. Eight of these were 'up' models, and the other eight were 'down'. A second group of 26 had energies between 318 and 367 kcal, and the remaining structures had energies between 407 and 470 kcal. Only the group with energies of about 240 kcal is relatively homogeneous in energy and hydroxyl orientation. That homogeneity is an additional confirmation that the lowest-energy group represents the most likely structures. Table 1 shows that the best 'up' model has an energy of 237.6 kcal, whereas the best 'down' model has an energy of 236.7 kcal. These values can be compared to the energy of the minimized, tetramer-based model of Sarko et al., 340.3 kcal. Tables S4 and S5 contain the Cartesian coordinates for the best up and down models.

Torsion angles were determined for the hydroxyl orientations of the central cellobiose units in the minicrystals.

Table 1. Energies (kcal) and hydroxyl torsion angles (°) for two central glucose residues from the best tetraose-based models

Model	Energy (kcal)	τ_2 (°)	τ_3 (°)	τ_6 (°)	$\tau_{2'}$ (°)	$\tau_{3'}$ (°)	$\tau_{6'}$ (°)
Starting	—	60.0	60.0	180.0	60.0	60.0	180.0
Best 'up'	237.6	12.2	−47.2	−138.9	12.0	−48.0	−140.0
Best 'down'	236.7	12.0	−48.0	−139.5	12.2	−47.2	−140.0

Variations in the torsion angles for the hydroxyl groups on the minicrystal surfaces result from the environments different than in the crystal interior. They are among the edge effects. The different starting orientations lead to different surface orientations and are the main factor responsible for the 9 kcal range of energies within the group that has the lowest energy. Because the energies are for all 26 cellobiose residues and 52 methyl groups in the minicrystal, the differences within the lowest-energy group are small per cellobiose unit.[†] We could not choose between the 'up' and 'down' models in the lowest-energy group, given such small energy differences.

The interior hydroxyl groups of the 16 lowest-energy structures rotated to nearly identical orientations during minimization even though they were in model crystal lattices. The H–C-2–O-2–H torsions (τ_2 and $\tau_{2'}$) were 12 ± 5°, H–C-3–O-3–H values (τ_3 and $\tau_{3'}$) were −47 ± 2°, and C-5–C-6–O-6–H torsions (τ_6 and $\tau_{6'}$) were −143 ± 3° regardless of the 'up' or 'down' packing or initial hydroxyl orientation. For example, the hydroxyl groups on C-2 and C-2′ rotated from initial values of 60° to final values near 12°, a rotation of 48°. Hydroxyl groups on C-2 of other structures in the low-energy group rotated to the same values near 12° starting from −60°, a rotation of 72°. The corresponding rotations at C-3 and C-6 of the lowest-energy structure were more than 107° and more than 40°, respectively. Hydroxyl groups on C-6 atoms in other structures in the lowest-energy group started at −60° and rotated about 72°. The extents of rotation of the hydroxyl groups were surprising since they were initially in staggered positions, normally considered to be energy minima, although nearly eclipsed conformations, such as the 12° torsion for O-2–H, are fairly common in carbohydrates and cyclitols. Such large rotations during minimization indicate that the attractiveness of the hydrogen-bond system was so great that the hydroxyl groups overcame energy barriers. The similarity of the unprimed and primed torsion angles in Table 1 strongly supports the experimentally determined twofold screw-axis symmetry.

[†]To get a rough lower limit on the energy difference per cellobiose unit, the energy difference between the up and down values could be divided by 26. Energy differences per cellobiose for the models based on cellohexaose (see below) could be divided by 39, and the comparable value for cellobiose in the cellobiose layer would require division by 13. Actual values would be somewhat larger because this calculation includes all surrounding molecules for only three of the central molecules of the minicrystal.

Unit-cell dimensions were assessed based on the interchain distances and angles. Those that were based on tetramer models were approximately $a = 4.5 \pm 0.09$ Å, $b = 8.0 \pm 0.1$ Å, $c = 10.35 \pm 0.03$ Å, $\alpha = 90.1 \pm 2°$, $\beta = 90.0 \pm 1.0°$, and $\gamma = 105.5 \pm 0.4°$ for the minimized models. Comparisons with the experimental values listed in Table 2 were satisfactory. Our minimized version of the model of Sarko et al.[10] gave $a = 10.44$ Å, $b = 7.95$ Å, $c = 10.36$ Å, $\alpha = 90.3°$, $\beta = 89.8°$, $\gamma = 122.85°$. Differences from the experimental values in Table 2 were also considered minor. The slight expansion of the unit cells, particularly along the *a*-axis, may be partly due to the lack of long-range packing forces in the minicrystals.

Although our lowest-energy values for the tetramer-based models of 237 kcal for the Wada et al. structure[9] and 340 kcal for the Sarko et al.[10] structure strongly favored the single-chain unit cell of Wada et al., there was concern regarding chain-end effects of unknown magnitude. The central chain in the two-chain model is displaced 0.9 Å along the *c*-axis with respect to the corner chains. Therefore, its minicrystal energies would be susceptible to end effects. In the case of the minicrystals of the one-chain cell, all chain-ending methyl groups are in planes at the tops and bottoms of the minicrystals. Because of the shifting in the two-chain cell, its chain ends would not experience the same degree of stabilization from van der Waals attraction to their neighbors as would the coplanar ends in the one-chain cell models. That problem was solved by comparing the energies of internal cellobiose layers in minicrystals built from cellohexaose molecules that had terminal methyl groups. The energies for the cellobiose layer were based on subtraction of the energies of the best 'up' and 'down' methylated cellotetraose minicrystals from energies of analogous methylated cellohexaose minicrystals. Those cellobiose layer energies, which do not have first-order end effects, are shown for the one- and two-chain cell structures in Table 2, along with the unit-cell dimensions of the models based on the cellohexaose molecules. In this case, the energies of the 'up' structure, both the full hexameric minicrystal and the cellobiose layer in the minicrystal, were slightly lower than those of its 'down' counterpart, but considerably lower than those of the two-chain cell structures.

Table 3 shows the geometries of the hydrogen bonds in which the central cellobiose unit in the minicrystal is involved, based on the hexameric models. Based on the criterion that the distance between the donated hydrogen and the acceptor oxygen atom is <3.0 Å and

Table 2. Calculated energies and unit-cell dimensions of hexamer models

Hexamer model	Minicrystal energy (kcal)	Cellobiose layer energy (kcal)	*a* (Å)	*b* (Å)	*c* (Å)	*α* (°)	*β* (°)	*γ* (°)
Best 'up' one-chain	322.2	84.5	4.58	7.95	10.33	90.3	90.1	107.9
Best 'down' one-chain	323.2	86.5	4.58	8.00	10.31	90.2	90.1	107.9
Wada et al.[9a]	—	—	4.45	7.85	10.31	90.0	90.0	105.1
Two-chain	477.5	137.2	10.45	7.92	10.33	90.2	89.8	122.8
Sarko et al.[10a]	—	—	10.25	7.78	10.34	90.0	90.0	122.4

[a] Experimentally determined.

Table 3. Intra- and inter-molecular[a] hydrogen bonds in best 'up' model

Type of bond	H bond	Length H···O (Å)	Length O···O (Å)	Angle (°)
Intramolecular	O-3H···O-5	1.92	2.73	142.4
	O-3H···O-6	2.38	3.07	129.2
	O-3H···O-4	2.77	3.00	94.6
Intermolecular				
Central chain donor	O-2H···O-6b	1.82	2.76	169.3
	O-2H′···O-6c′	1.82	2.75	168.3
	O-6H···O-2d	1.79	2.72	163.1
	O-6H′···O-2a′	1.80	2.73	164.6
Central chain acceptor	O-6Ha···O-2	1.79	2.71	163.2
	O-2Hc···O-6	1.81	2.74	167.6
	O-2b′···O-6′	1.81	2.74	166.8
	O-6Hd′···O-2′	1.79	2.72	165.0

[a] Letters a, b, c, and d refer to neighboring glucose residues with the same *z*-coordinates as the central residue. See Figure 3.

the O–H···O angle is >90°, there are three intramolecular and two intermolecular hydrogen bonds.

The intramolecular hydrogen bonds, shown in Figure 3, are typical for β-(1→4) linked carbohydrates.[17] The proton of the O-3 hydroxyl group is positioned to donate to the O-5′ atom (see Fig. 3) by virtue of the particular ϕ and ψ linkage torsion-angles. The O-6′ atom also accepts from O-3–H. That frequently overlooked interaction stabilizes the *gt* position in many related molecules, despite H···O distances that are longer than are often considered to be hydrogen bonds.[18] The third intramolecular interaction in Table 3, O-3–H···O-4 is indeed very weak, but its presence is noted.

Although Table 3 shows four intermolecular hydrogen bonds in which the central cellobiose is the donor and four hydrogen bonds in which it is the acceptor, there is just one unique O-6–H···O-2 hydrogen bond and one O-2–H···O-6 hydrogen bond when there is actual twofold symmetry. The near identity of these modeled geometries for the O-6–H···O-2 hydrogen bonds confirms that the twofold, single-chain structure is consistent with the MM3 force field. The O-2–H···O-6 geometries lead to a similar conclusion.

The intermolecular hydrogen bonds participate in 'infinite' chains of donor–acceptor–donor linkages (Fig. 3) that have excellent hydrogen-bonding geometry. Such systems have increased strength and shortened interatomic distances because of the phenomenon of 'cooperativity'.[19]

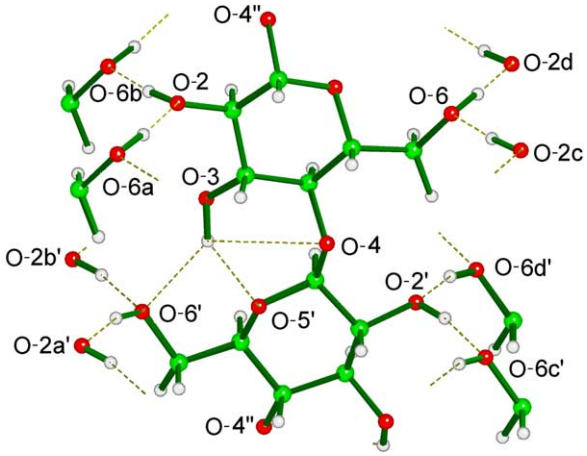

Figure 3. Hydrogen bonding in cellulose III_I. The central cellobiose unit of the best 'up' minicrystal based on cellohexaose is shown along with hydroxyl and hydroxymethyl groups from the four neighboring cellobiose units, a–d. Groups from the a and c chains are in front of the central cellobiose, and those from the b and d chains are behind it. Hydrogen bonds are shown as dashed lines. The O-6 and O-2 atoms participate in infinite chains of donor···acceptor···donor hydrogen bonds, indicated by the dashed lines that would connect to cellobiose units in front of, and behind, the central cellobiose unit.

van der Waals forces are also important, with stacking of the residues in the *a*-axis direction. Each of the methine hydrogen atoms is in van der Waals contact with one or more methine hydrogen atoms on the

neighboring molecules. Figure 4 illustrates the H···H distances <3.2 Å for the best 'up' model.

Our best 'up' model is similar in many respects to the high-resolution structure very recently published by Wada et al.[11] Interestingly, they were able to clearly rule out the 'down' packing model, while our results are ambiguous on that point. The conformations of the primary alcohol groups (O-5–C-5–C-6–O-6 torsion angles) in the experiment and model are 44° and 59°, respectively. Despite that difference, the resulting positions of the O-6 hydroxyl hydrogens are quite similar. The biggest difference is in the positions of the two protons attached to C-6. These relationships are shown in Figure 5, in which the central cellobiose unit from the hexaose-based 'up' minicrystal is fitted to a cellobiose unit generated from the coordinates of Wada et al.[11] The root mean square difference between the positions of the 12 ring atoms and the linkage oxygen is only 0.1 Å.

In the high-resolution structure of Wada et al.,[11] there was one slight ambiguity regarding the direction of the infinite cooperative hydrogen-bonding network. Although their final result was quite similar to ours, they also considered an alternative that reversed the direction of the donor and acceptor hydroxyl groups. In the agreed upon network, our O-2 hydroxyls have 12° torsion angles, nearly eclipsing the C-2–H hydrogen atoms. In the alternative network structure, the O-2–H atoms are oriented anti to the C-2–H hydrogens. Experimentally, this ambiguity arises because of the difficulty in precisely locating the proton between two oxygen atoms. If it is closer to O-2, then it is taken to be covalently bonded to O-2 and hydrogen bonded to O-6, and vice versa. In a structural or modeling sense, direction of the hydrogen bonding in an infinite network is expressed by the rotational orientation of the hydroxyl groups. The modeling results were less ambiguous, because the various torsional and other steric terms in the force field result in the alternative systems being considerably higher

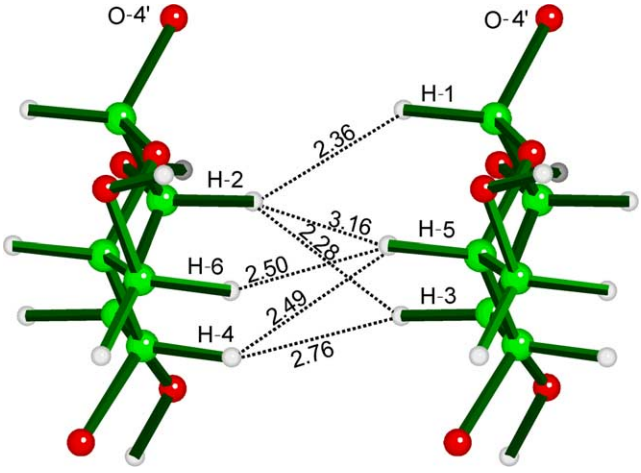

Figure 4. Two glucose residues from the center of the best 'up' hexameric minicrystal, showing the H···H contacts <3.2 Å.

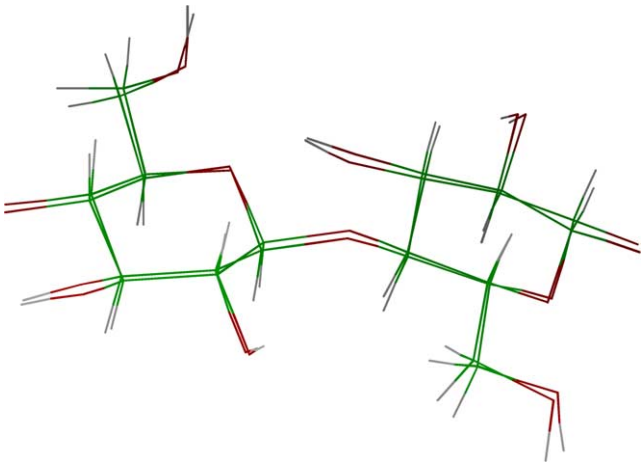

Figure 5. Superimposed cellobiose units from the experimental structure of Wada et al.[11] and the best 'up' model. The root mean square fit for the ring atoms and central linkage oxygen is 0.1 Å.

in energy. Several minicrystals having the alternative hydrogen-bonding scheme fell into the second lowest-energy group. Thus, the alternative scheme was rejected by both the modeling and by the neutron-diffraction results, but more strongly by the modeling.

To understand why Sarko et al. proposed a two-chain structure, we reviewed their published (as supplementary data) crystallographic information and recorded a fiber-diffraction pattern of ramie cellulose III_I prepared by the method of Yatsu et al.[20] All of the diffraction spots on our low-resolution pattern could be indexed with the one-chain cell. All but two of their spots on the first-layer line (*d*-spacings = 2.78 and 2.55 Å) could also be indexed with the one-chain cell. Those spots were not visible on our pattern. Their published pattern does not permit a close analysis, but one plausible explanation, that traces of cellulose I remained, is not likely because there is no 2.78 Å observed *hk*1 spacing from cellulose I.[21] It appears that Sarko et al. assumed that there were two chains in the cell. Ironically, Sarko and Muggli had earlier discussed a one-chain unit cell for cellulose I before the distinction between cellulose Iα and Iβ was understood.[22] In any case, the synchrotron fiber-diffraction pattern by Wada et al. produced 114 reflections that were indexed by the proposed one-chain monoclinic unit cell, compared to the 23 reflections in the earlier work. The cell based on the larger number of reflections would normally overrule one based on the much smaller number of spots. In the present situation, one must be careful about such an assumption, given that the starting cellulose came from two different sources in the two experiments.

4. Conclusions

Our modeling study of cellulose III_I concurs that the one-chain unit cell of Wada et al., with O-6 in the *gt*

position, is more probable than the previous two-chain cell of Sarko et al., which had O-6 in *tg* positions. Furthermore, the resemblance between the model up chains and the experimental structure was close enough to understand the important aspects of the structure. On the other hand, our best 'up' and 'down' models showed very small differences between them, either in the energies, the unit-cell dimensions, or the hydrogen-bond geometries, and so were ambiguous on that point. Again on the positive side, the modeling method gave a strong preference for the direction of the interchain hydrogen bonding, a point with some small ambiguity in the experimental work. Most surprising to us was the extent of motion of the hydroxyl groups to establish the correct hydrogen-bonding system.

Acknowledgements

Elena Graves and Dr. Ralph Berni prepared the cellulose III sample, and Dr. Paul Langan participated in helpful discussions. Dr. Henry Bellamy gave assistance and advice on the synchrotron data collection. The cellulose III diffraction pattern was recorded at the Gulf Coast Protein Crystallography Consortium beamline at the Center for Advanced Microstructures and Devices, Baton Rouge, LA.

Supplementary data

Supplementary data associated with this article can be found, in the online version, at doi:10.1016/j.carres.2005.01.028. A link via a footnote on the first page to the Supplementary Material is provided in ScienceDirect.

References

1. Jones, D. W. *J. Polym. Sci.* **1960**, *42*, 173–188.
2. Smith, P. J. C.; Arnott, S. *Acta Crystallogr., Sect. A* **1978**, *34*, 3–11.
3. Motherwell, W. D.; Ammon, H. L.; Dunitz, J. D.; Dzyabchenko, A.; Erk, P.; Gavezzotti, A.; Hofmann, D. W.; Leusen, F. J.; Lommerse, J. P.; Mooij; Price, S. L.; Scheraga, H.; Schweizer, B.; Schmidt, M. U.; van Eijck, B. P.; Verwer, P.; Williams, D. E. *Acta Crystallogr., Sect. B* **2002**, *58*, 647–661.
4. Nishiyama, Y.; Kuga, S.; Wada, M.; Okano, T. *Macromolecules* **1997**, *56*, 6395–6397.
5. Nishiyama, Y.; Sugiyama, J.; Chanzy, H.; Langan, P. *J. Amer. Chem. Soc.* **2003**, *125*, 14300–14306.
6. Nishiyama, Y.; Langan, P.; Chanzy, H. *J. Am. Chem. Soc.* **2002**, *124*, 9074–9082.
7. Langan, P.; Nishiyama, Y.; Chanzy, H. *Biomacromolecules* **2001**, *2*, 410–416.
8. Wada, M.; Heux, L.; Sugiyama, J. *Biomacromolecules* **2004**, *5*, 1385–1391.
9. Wada, M.; Heux, L.; Isogai, A.; Nishiyama, Y.; Chanzy, H.; Sugiyama, J. *Macromolecules* **2001**, *34*, 1237–1243.
10. Sarko, A.; Southwick, J.; Hayashi, J. *Macromolecules* **1976**, *9*, 857–863.
11. Wada, M.; Chanzy, H.; Nishiyama, Y.; Langan, P. *Macromolecules* **2004**, *37*, 8548–8555.
12. Ford, Z. M.; Stevens, E. D.; Johnson G. P.; French, A. D. Southeast Regional Meeting, American Chemical Society (ACS), Atlanta, Nov 17, 2003; ACS National Meeting, Anaheim, CA, March 27, 2004; CARB028.
13. Gardner, K. H.; Blackwell, J. *Biopolymers* **1974**, *13*, 1975–2001.
14. French, A. D.; Howley, P. S. Comparisons of Structures Proposed for Cellulose. In *Cellulose and Wood—Chemistry and Technology*; Scheurch, C., Ed.; Wiley and Sons: New York, 1989; pp 159–167.
15. French, A. D.; Miller, D. P.; Aabloo, A. *Int. J. Biol. Macromol.* **1993**, *15*, 30–36.
16. Mazeau, K.; Heux, L. *J. Phys. Chem. B* **2003**, *107*, 2394–2403.
17. French, A. D.; Johnson, G. P. *Cellulose* **2004**, *11*, 5–22.
18. Peralta-Inga, Z.; Johnson, G. P.; Dowd, M. K.; Rendleman, J. A.; Stevens, E. D.; French, A. D. *Carbohydr. Res.* **2002**, *237*, 851–861.
19. Jeffrey, G. A.; Saenger, W. *Hydrogen Bonding in Biological Structures*; Springer: Berlin, 1991; p 35 and other pages therein.
20. Yatsu, L. Y.; Calamari, T. A., Jr.; Benerito, R. R. *Text. Res. J.* **1986**, *56*, 419–424.
21. Mann, J.; Roldan-Gonzalez, L.; Wellard, H. J. *J. Polym. Sci.* **1960**, *42*, 165–171.
22. Sarko, A.; Muggli, R. *Macromolecules* **1974**, *7*, 486–494.